Precision tests of Quantum Mechanics and CPT symmetry with entangled neutral kaons at KLOE

Riccardo D'Amico on behalf of the KLOE-2 collaboration

Kaon Interferometry at a ϕ-factory

From the strong decay of the vector meson
$\phi^{C=P=-1}$ $(BR(\phi \to K^0\overline{K}^0) \approx 34\%)$.
$\Delta t = |t_1 - t_2|$

Kaon Interferometry at a ϕ-factory

From the strong decay of the vector meson $\phi^{C=P=-1}$ ($BR(\phi \to K^0\overline{K}^0) \approx 34\%$).

$\Delta t = |t_1 - t_2|$

$$|i\rangle = \frac{1}{\sqrt{2}}[\,|K^0\rangle|\overline{K}^0\rangle - |\overline{K}^0\rangle|K^0\rangle]$$

Kaon Interferometry at a ϕ-factory

From the strong decay of the vector meson $\phi^{C=P=-1}$ ($BR(\phi \to K^0\overline{K}^0) \approx 34\%$).

$\Delta t = |t_1 - t_2|$

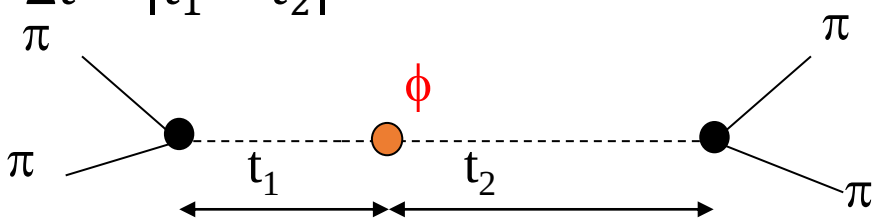

$$|i\rangle = \frac{1}{\sqrt{2}}[\,|K^0\rangle|\overline{K}^0\rangle - |\overline{K}^0\rangle|K^0\rangle]$$

$$I(\pi^+\pi^-\pi^+\pi^-;\Delta t) \propto e^{-\Gamma_S \Delta t} + e^{-\Gamma_L \Delta t} - 2\, e^{-\frac{\Gamma_S+\Gamma_L}{2}\Delta t}\cos(\Delta m \Delta t)$$

Kaon Interferometry at a ϕ-factory

From the strong decay of the vector meson $\phi^{C=P=-1}$ ($BR(\phi \to K^0\bar{K}^0) \approx 34\%$).

$\Delta t = |t_1 - t_2|$

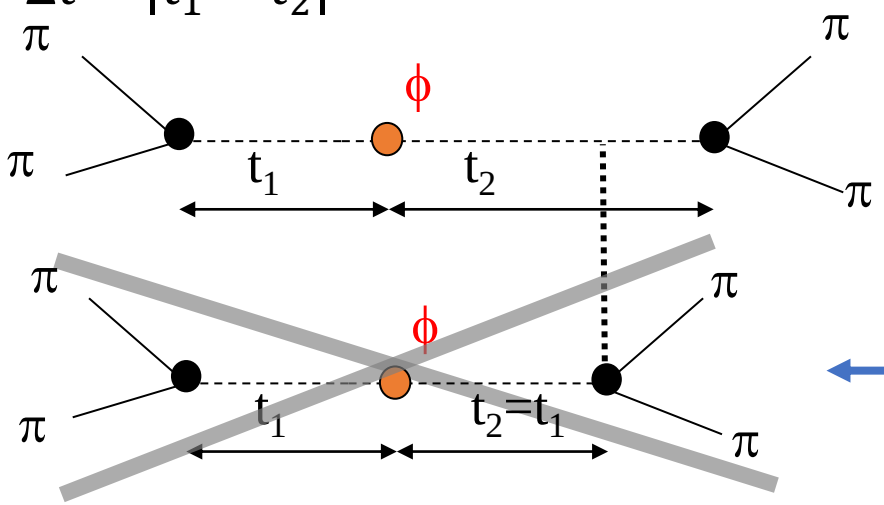

$$|i\rangle = \frac{1}{\sqrt{2}}[\,|K^0\rangle|\bar{K}^0\rangle - |\bar{K}^0\rangle|K^0\rangle]$$

$$I(\pi^+\pi^-\pi^+\pi^-;\Delta t) \propto e^{-\Gamma_S \Delta t} + e^{-\Gamma_L \Delta t} - 2\, e^{-\frac{\Gamma_S+\Gamma_L}{2}\Delta t}\cos(\Delta m \Delta t)$$

$I(\pi^+\pi^-\pi^+\pi^-;\Delta t) = 0$ when $\Delta t = 0$.

No simultaneous decay in the same final states.

Decoherence and CPT violation

Most precise test of quantum coherence in an entangled system:

- Search for decoherence effect;

Decoherence and CPT violation

Most precise test of quantum coherence in an entangled system:

- Search for decoherence effect;

$$I(\pi^+\pi^-,\pi^+\pi^-;\Delta t) = \frac{N}{2}\left[\left|\langle\pi^+\pi^-,\pi^+\pi^-|K^0\bar{K}^0(\Delta t)\rangle\right|^2\left|\langle\pi^+\pi^-,\pi^+\pi^-|\bar{K}^0K^0(\Delta t)\rangle\right|^2 - (1-\zeta_{0\bar{0}})\cdot 2\Re\left(\langle\pi^+\pi^-,\pi^+\pi^-|K^0\bar{K}^0(\Delta t)\rangle\langle\pi^+\pi^-,\pi^+\pi^-|\bar{K}^0K^0(\Delta t)\rangle^*\right)\right.$$

$\zeta_{0\bar{0}}$ decoherence parameter in the $K^0\bar{K}^0$ basis (QM predicts: $\zeta_{0\bar{0}} = 0$).
[or ζ_{SL} in the K_SK_L basis].

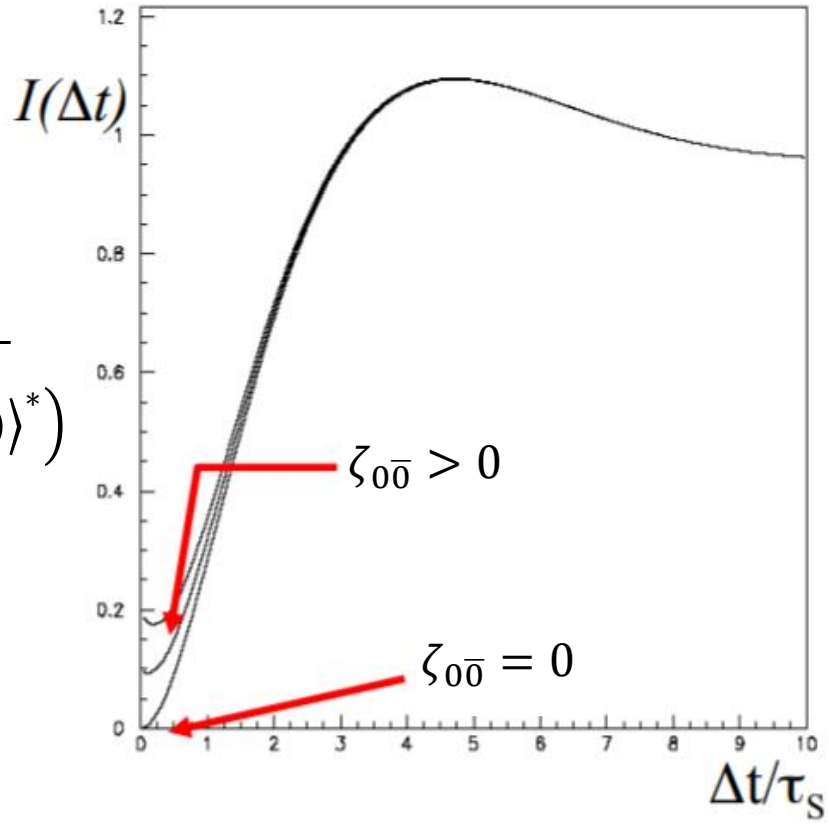

Decoherence and CPT violation

Decoherence effects might arise in a quantum gravity picture necessarily entailing CPT violation [Ellis et. al, NP B241 (1984) 381 (*); Ellis, Mavromatos et al. PRD53 (1996) 3846 (**)]:

- In this case the relevant parameter in the modified time evolution of neutral kaons is the γ parameter (at most $\gamma = O(m_K^2 / M_{planck}) \approx 2x10^{-20}$ GeV).
- the initial entangled state is modified adding a tiny symmetric part $\rightarrow \omega$ effect (at most $\omega = O(m_K^2 / M_{planck}/\Delta\Gamma) \sim 1x10^{-3}$)

* https://doi.org/10.1016/0550-3213(84)90053-1

** https://doi.org/10.1103/PhysRevD.53.3846

Decoherence and CPT violation

Decoherence effects might arise in a quantum gravity picture necessarily entailing CPT violation [Ellis et. al, NP B241 (1984) 381 (*); Ellis, Mavromatos et al. PRD53 (1996) 3846 (**)]:

- In this case the relevant parameter in the modified time evolution of neutral kaons is the γ parameter (at most $\gamma = O(m_K^2 / M_{planck}) \approx 2x10^{-20}$ GeV).
- the initial entangled state is modified adding a tiny symmetric part $\rightarrow$ ω effect (at most $\omega = O(m_K^2 / M_{planck}/\Delta\Gamma) \sim 1x10^{-3}$)

$$|i\rangle \propto \frac{1}{\sqrt{2}}[\,|K^0\rangle|\bar{K}^0\rangle - |\bar{K}^0\rangle|K^0\rangle] + \omega[\,|K^0\rangle|\bar{K}^0\rangle + |\bar{K}^0\rangle|K^0\rangle] \longrightarrow \text{[in the } K^0\bar{K}^0 \text{ basis]}$$

* https://doi.org/10.1016/0550-3213(84)90053-1

** https://doi.org/10.1103/PhysRevD.53.3846

Decoherence and CPT violation

Decoherence effects might arise in a quantum gravity picture necessarily entailing CPT violation [Ellis et. al, NP B241 (1984) 381 (*); Ellis, Mavromatos et al. PRD53 (1996) 3846 (**)]:

- In this case the relevant parameter in the modified time evolution of neutral kaons is the γ parameter (at most $\gamma = O(m_K^2 / M_{planck}) \approx 2x10^{-20}$ GeV).
- the initial entangled state is modified adding a tiny symmetric part $\rightarrow \omega$ effect (at most $\omega = O(m_K^2 / M_{planck}/\Delta\Gamma) \sim 1x10^{-3}$)

$$|i\rangle \propto \frac{1}{\sqrt{2}}[\,|K^0\rangle|\bar{K}^0\rangle - |\bar{K}^0\rangle|K^0\rangle] + \omega[\,|K^0\rangle|\bar{K}^0\rangle + |\bar{K}^0\rangle|K^0\rangle] \longrightarrow$$ [in the $K^0\bar{K}^0$ basis]

[in the $K_S K_L$ basis] $\longleftarrow$ $|i\rangle \propto [\,|K_S\rangle|K_L\rangle - |K_L\rangle|K_S\rangle] + \omega[\,|K_S\rangle|K_S\rangle - |K_L\rangle|K_L\rangle\,]$

* https://doi.org/10.1016/0550-3213(84)90053-1

** https://doi.org/10.1103/PhysRevD.53.3846

The KLOE detector

KLOE detector

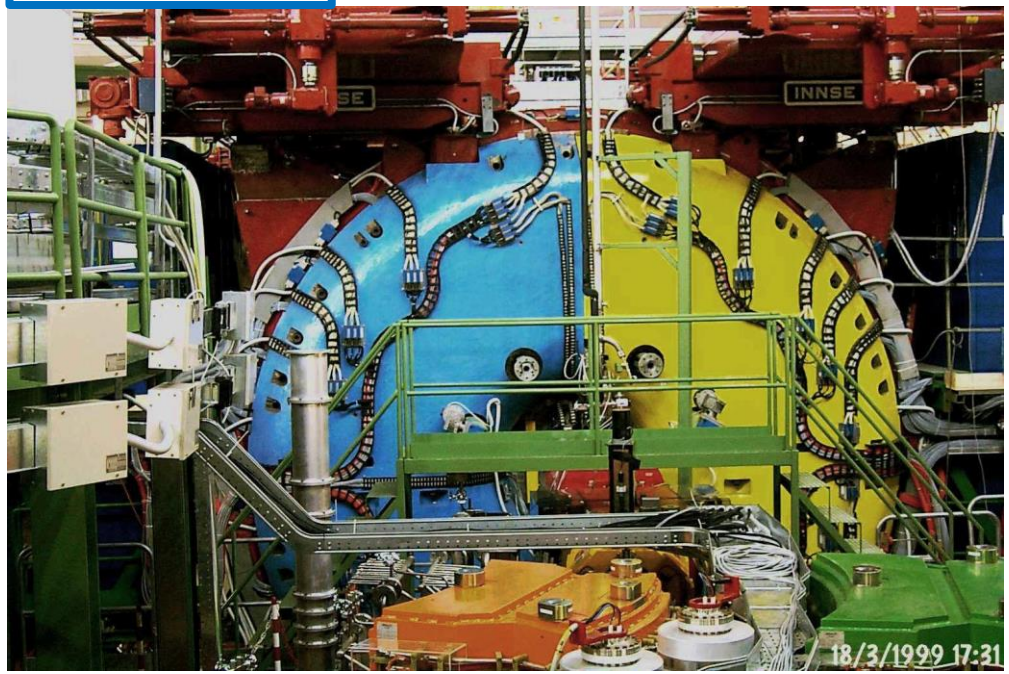

DAϕNE e^+e^- **collider. Frascati, Italy.**

The KLOE detector

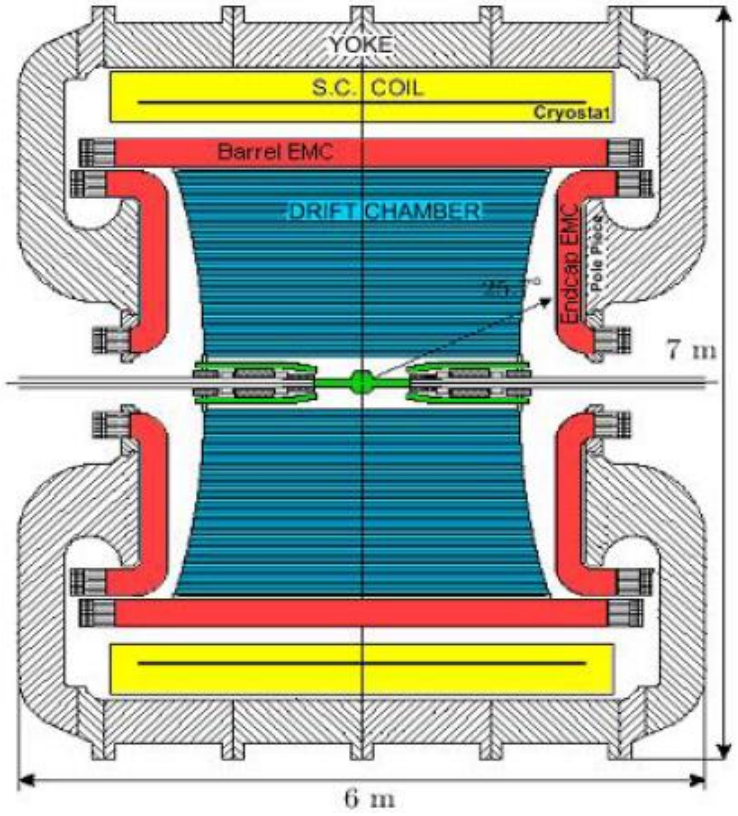

The KLOE detector

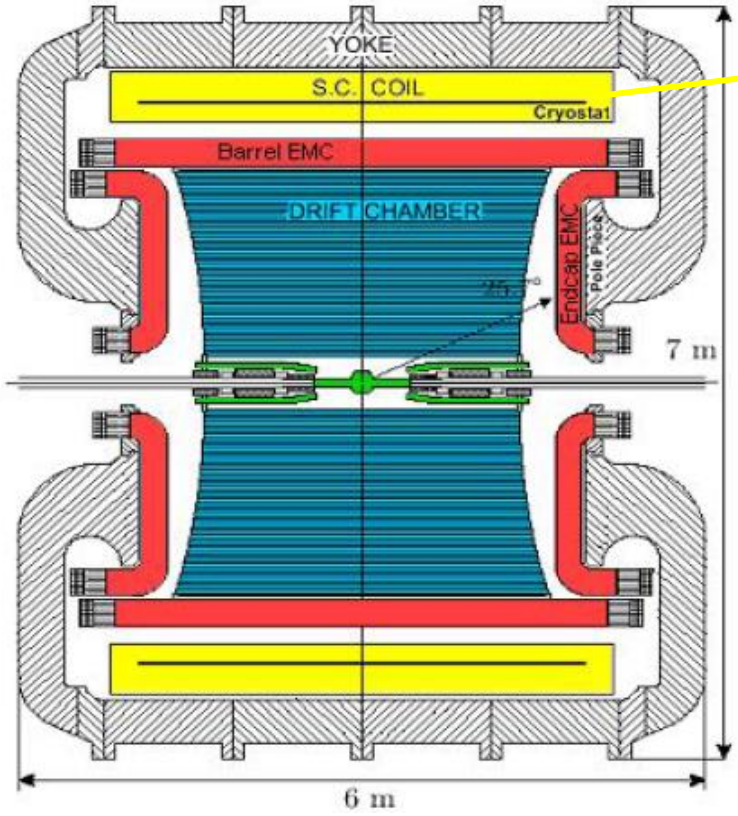

Super Conductive Coil:
$\mathrm{B} = 0.52\ T$

The KLOE detector

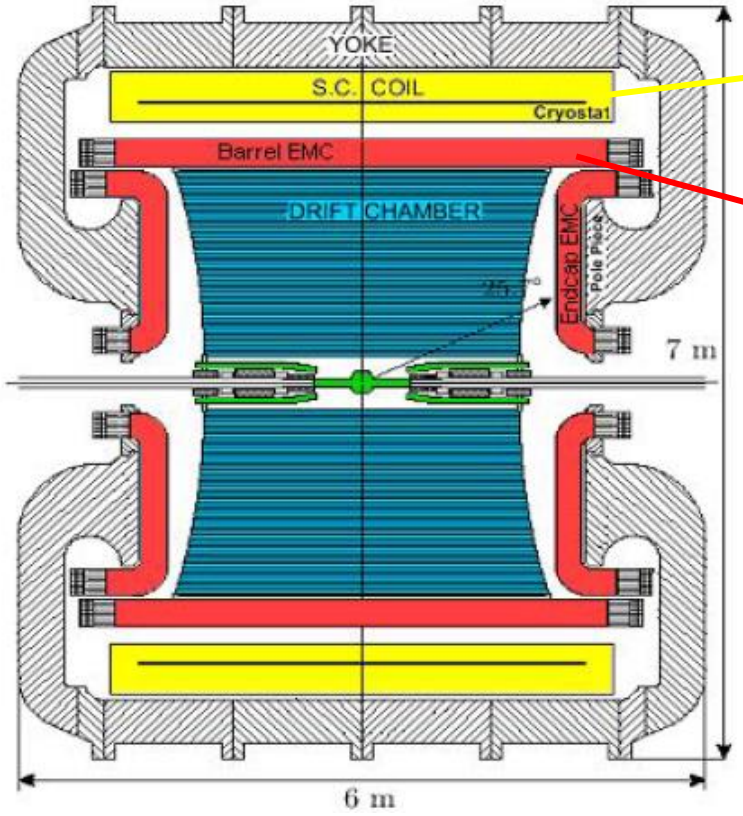

Super Conductive Coil:
$B = 0.52\ T$

Electromagnetic Calorimeter (lead scintillating fibers):

$$\frac{\sigma(E)}{E} = \frac{5.7\%}{\sqrt{E[GeV]}}$$

$$\sigma(t) = \frac{54ps}{\sqrt{E[GeV]}} \oplus 140\ ps$$

The KLOE detector

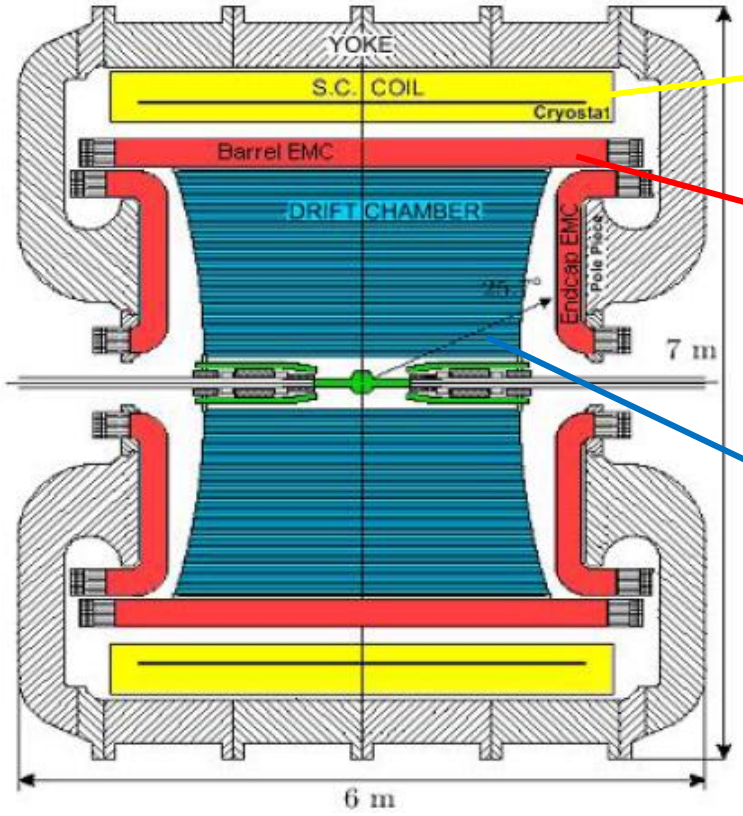

Super Conductive Coil:
$\mathrm{B} = 0.52\ T$

Electromagnetic Calorimeter (lead scintillating fibers):

$$\frac{\sigma(E)}{E} = \frac{5.7\%}{\sqrt{E[GeV]}}$$

$$\sigma(t) = \frac{54ps}{\sqrt{E[GeV]}} \oplus 140\ ps$$

Drift Chamber:
≈ 52000 wires (≈ 12500 sense wires);
$\approx 200\ \mu m$ resolution in the bending plane;
$\approx 1\ mm$ resolution on the decay vertex.
Gas mixture of $90\%\ He\ - 10\%\ iC_4H_{10}$

The KLOE detector

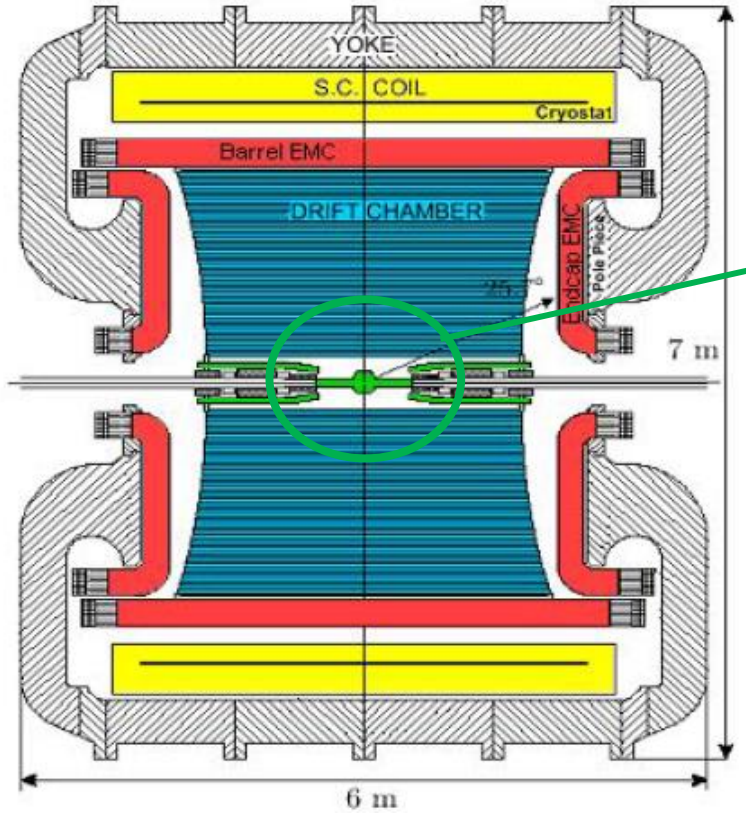

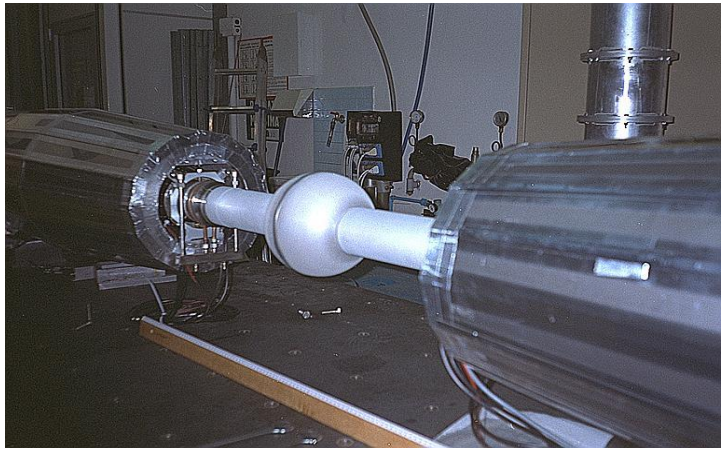

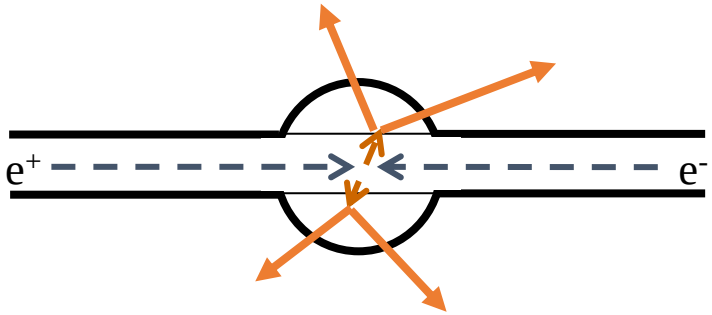

Beryllium cylindrical tube coaxial to the beam ($4.4\ cm$ radius $50\ \mu m$ thick) + Spherical Al/Be $38/62$ pipe ($10\ cm$ radius $0.5\ mm$ thick).

Event selection

The analysis was performed on the KLOE data corresponding to a luminosity $\boldsymbol{L \approx 1.7\ fb^{-1}}$.

Candidate signal events require two vertices with opposite curvature tracks each with at least one within a fiducial volume ($\rho < 10cm$, $|\mathrm{z}| < 20\mathrm{cm}$) centered at the collision point. Furthermore the following preselection criteria are applied:

- $|m_i(\pi^+\pi^-) - m_K| < 5\ MeV$, with $m(\pi^+\pi^-)$ the invariant mass of the tracks;
- $\left|\left|\vec{p}^{\,*}_{i+} + \vec{p}^{\,*}_{i-}\right| - p^*_K\right| < 10\ MeV$, with $\vec{p}_{i\pm}{}^*$ the pion momenta of the vertex *i* in the ϕ rest frame and p^*_K the Kaon momentum calculated from the $\phi \to K_S K_L$ cinematics,
- $-50 < E^2_{miss} - |\vec{p}_{miss}|^2 < 10\ MeV^2$, with $\vec{p}_{miss} = \vec{p}_\phi - \vec{p}_1 - \vec{p}_2$ and $E_{miss} = E_\phi - E_1 - E_2$
- $\sqrt{E^2_{miss} + |\vec{p}_{miss}|^2} < 10\ MeV.$

Kinematic Fit

A kinematic fit was performed to improve the resolution on the kaon decay vertices, parametrized as:

$$\vec{V}_i = \vec{V}_\phi + \lambda_i \hat{n}_i,$$

The kinematic fit solves λ_i and $\vec{V}_\phi$ by maximazing the log likelihood function:

$$\ln L = \sum_{i=1,2} lnP_i\left(\vec{V}_i^{\,rec} - \vec{V}_i^{\,fit}\right) + lnP_\phi\left(\vec{V}_\phi^{\,rec} - \vec{V}_\phi^{\,fit}\right)$$

Probability density functions representig the resolutions for the vertices as for the MC

All events with $-2\ln L < 30$ and $\frac{\left|\lambda_i^{fit} - \lambda_i^{reco}\right|}{\sigma\left(\lambda_i^{fit}\right)} < 10$ are retained.

Pion Angle Cut

Since the Δt resolution is strongly correlated with the opening angle $\theta_{\pi\pi}$ of the pion tracks, worsening for large values of the angle, a final selection cut is applied to candidate events requiring for both vertices $\cos(\theta_{\pi^+\pi^-}) > -0.975$

Pion Angle Cut

Since the Δt resolution is strongly correlated with the opening angle $\theta_{\pi\pi}$ of the pion tracks, worsening for large values of the angle, a final selection cut is applied to candidate events requiring for both vertices $\cos(\theta_{\pi^+\pi^-}) > -0.975$

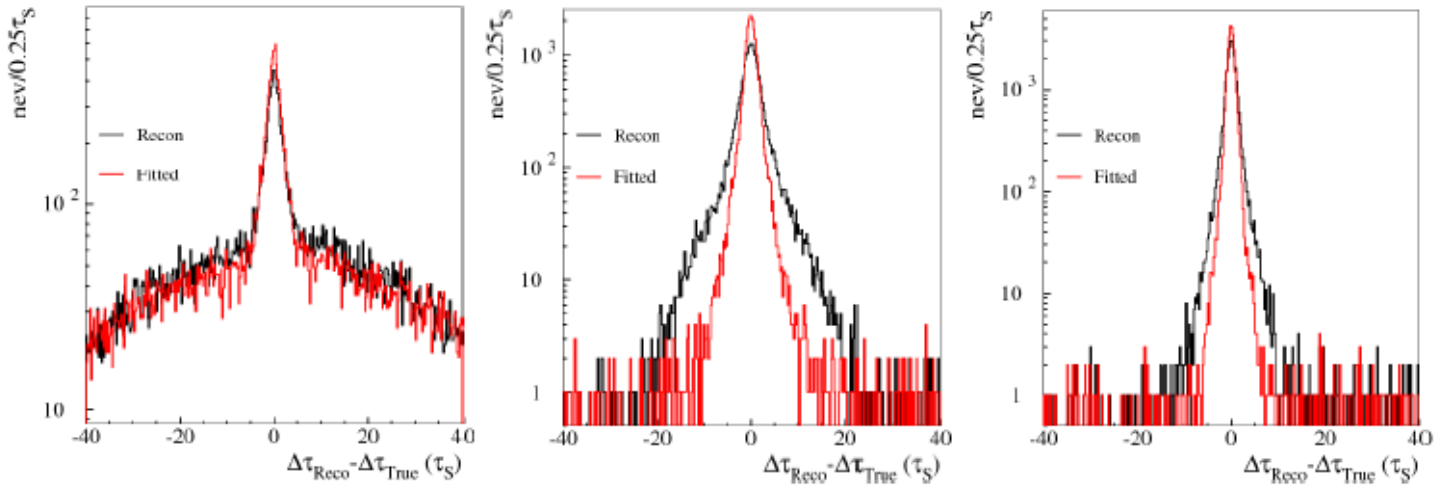

Pion Angle Cut

Since the Δt resolution is strongly correlated with the opening angle $\theta_{\pi\pi}$ of the pion tracks, worsening for large values of the angle, a final selection cut is applied to candidate events requiring for both vertices $\cos(\theta_{\pi^+\pi^-}) > -0.975$

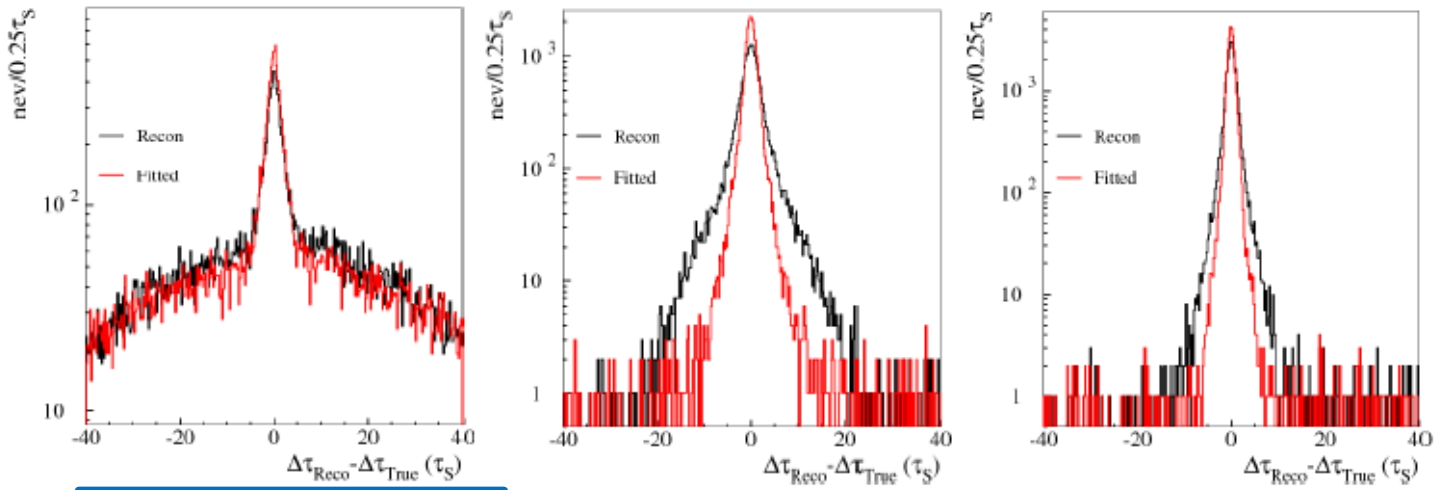

$-1 < \cos(\theta_{\pi\pi}) < -0.99$

Pion Angle Cut

Since the Δt resolution is strongly correlated with the opening angle $\theta_{\pi\pi}$ of the pion tracks, worsening for large values of the angle, a final selection cut is applied to candidate events requiring for both vertices $\cos(\theta_{\pi^+\pi^-}) > -0.975$

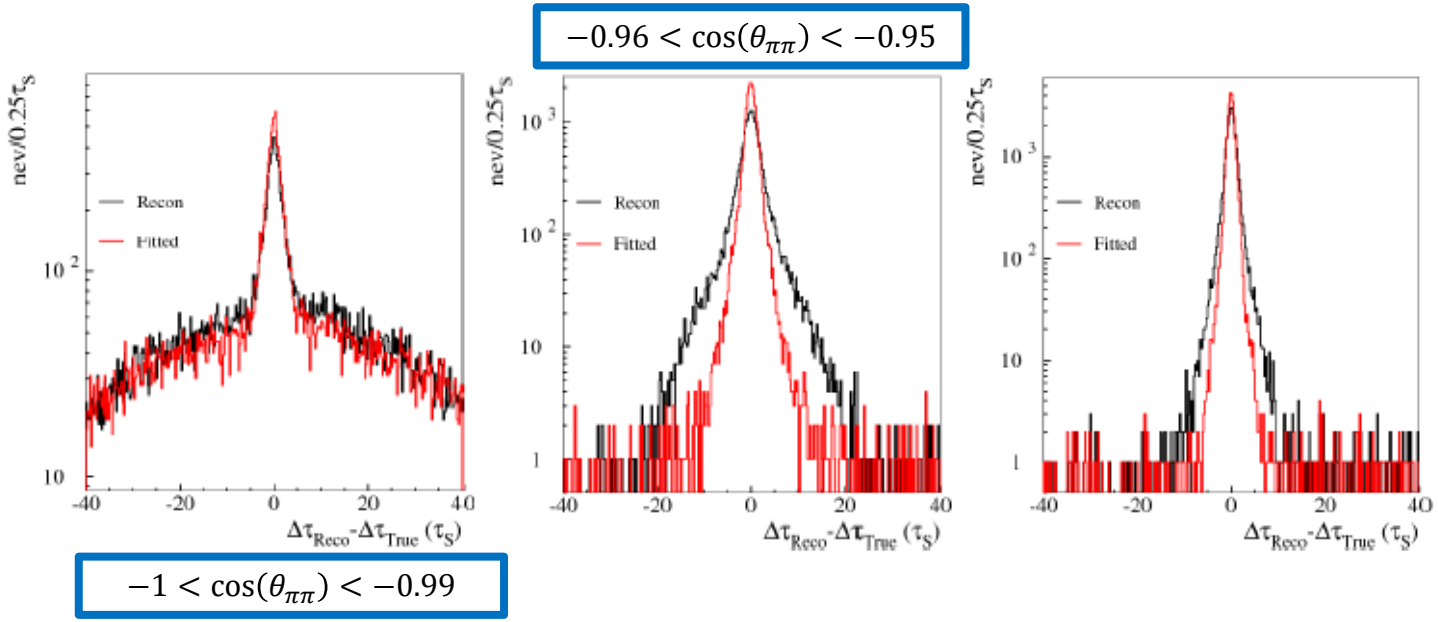

Pion Angle Cut

Since the Δt resolution is strongly correlated with the opening angle $\theta_{\pi\pi}$ of the pion tracks, worsening for large values of the angle, a final selection cut is applied to candidate events requiring for both vertices $\cos(\theta_{\pi^+\pi^-}) > -0.975$

$-0.96 < \cos(\theta_{\pi\pi}) < -0.95$

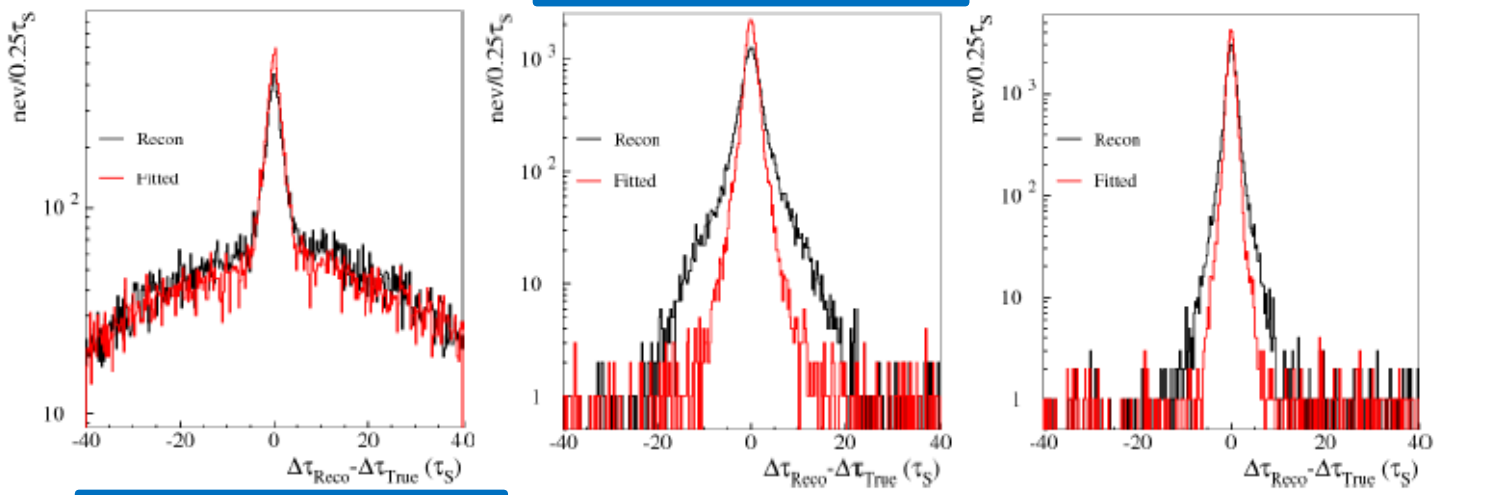

$-1 < \cos(\theta_{\pi\pi}) < -0.99$

$-0.89 < \cos(\theta_{\pi\pi}) < -0.88$

Background evaluation

Two main background sources:

- Non-resonant production of four pions, $e^+e^- \rightarrow \pi^+\pi^-\pi^+\pi^-$, non dominant (0.5% in the $0 < \Delta t < 12\tau_S$ range) but concentrated at $\Delta t \approx 0$.
- K_S regeneration in the beam pipe.

The remaining background due to semileptonic K_L decay can be considered negligible, being uniformely distributed in Δt and amounting (from the MC) to less than 0.2% in the chosen fit range.

$e^+e^- \to \pi^+\pi^-\pi^+\pi^-$ Background

Evaluated by studying the two-dimensional invariant mass distribution of the reconstructed kaon vertices in bins of Δt.

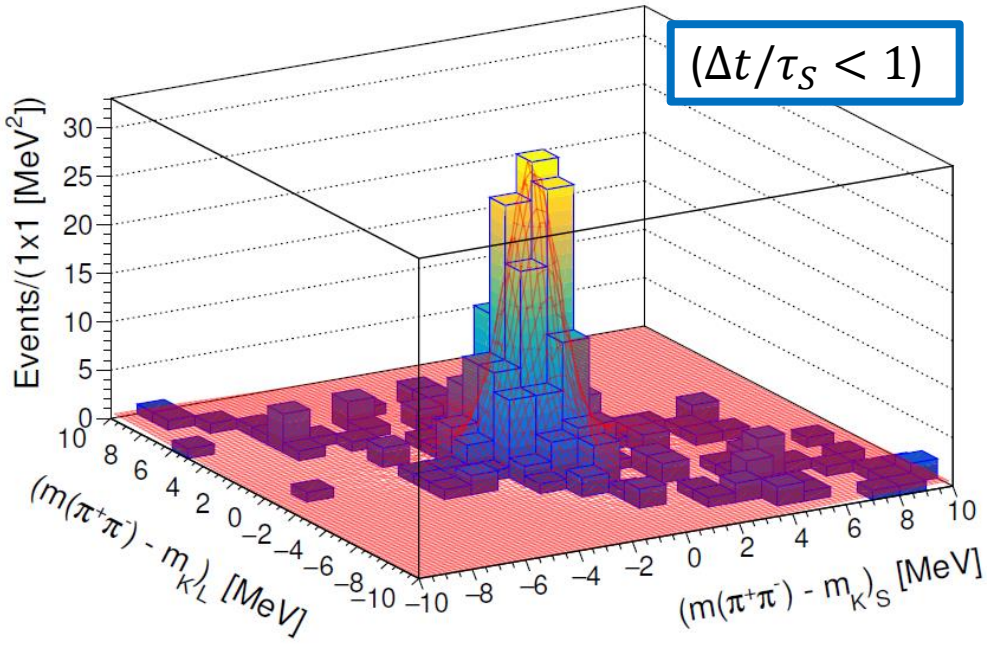

An unbinned maximum likelihood fit was performed in order to evaluate the number of events with the following model:

$$N_{obs}(x,y) = N_S \cdot S(x,y) + N_B \cdot G(z;\mu_z = 0\,,\sigma_B)$$

With $x, y = [m(\pi^+\pi^-) - m_K]_{S,L}$, $S(x,y)$ the template for the signal shape obtained from MC after selection, $G(z;\mu_z = 0\,,\sigma_B)$ a Gaussian distribution as a function of the variable $z = x + y$ with zero mean ($x = -y$) and standard deviation σ_B as free parameter of the fit.

$e^+e^- \to \pi^+\pi^-\pi^+\pi^-$ Background

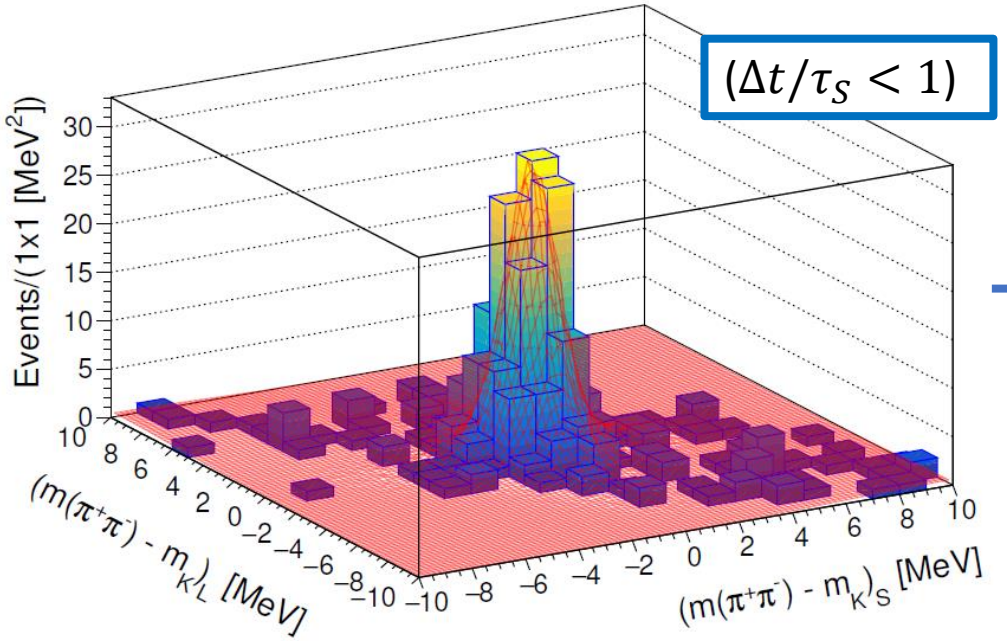

$$N_{bkg(\Delta t/\tau_S<1)} = 39 \pm 5$$
$$N_{bkg(1<\Delta t/\tau_S<2)} = 6 \pm 2$$
$$N_{bkg(2<\Delta t/\tau_S<3)} = 6 \pm 2$$

For $3 < \Delta t/\tau_s < 4$ it was found $N_{bkg} = 3 \pm 1$. From these results we conclude that the $e^+e^- \to \pi^+\pi^-\pi^+\pi^-$ can be considered negigible for $\Delta t > 3\tau_S$

Regeneration Background

- Peaks in the region $\Delta t \approx 17\ \tau_s$ due to the spherical beam pipe.
  - Fit region restricted in the range $0 < \Delta t < 12\tau_s$ to avoid this background
- Remaining background due to small contribution from the thin beryllium cylinder, dominated by incoherent over the coherent regeneration (neglected).

  The latter is evaluated with Monte Carlo, the K_S regeneration probability is extrapolated from the relation:

$$P_{reg}^{cyl} = D_{geom} \cdot P_{reg}^{sph} \cdot f(r)$$

Regeneration Background

- Peaks in the region $\Delta t \approx 17\ \tau_s$ due to the spherical beam pipe.
  - Fit region restricted in the range $0 < \Delta t < 12\tau_s$ to avoid this background
- Remaining background due to small contribution from the thin beryllium cylinder, dominated by incoherent over the coherent regeneration (neglected).

$$P_{reg}^{cyl} = D_{geom} \cdot P_{reg}^{sph} \cdot f(r)$$

Geometrical Factor

Measured regeneration probability in the spherical beam pipe

Cross section ratio for beryllium and aluminum

$$r = \frac{\sigma_{inc}(Be)}{\sigma_{inc}(Al)}$$

Regeneration Background

- Peaks in the region $\Delta t \approx 17\ \tau_s$ due to the spherical beam pipe.
  - Fit region restricted in the range $0 < \Delta t < 12\tau_s$ to avoid this background
- Remaining background due to small contribution from the thin beryllium cylinder, dominated by incoherent over the coherent regeneration (neglected).

The regeneration correction factor is obtained by the ratio between the MC histogram distributions with and without the regeneration.

Efficiencies

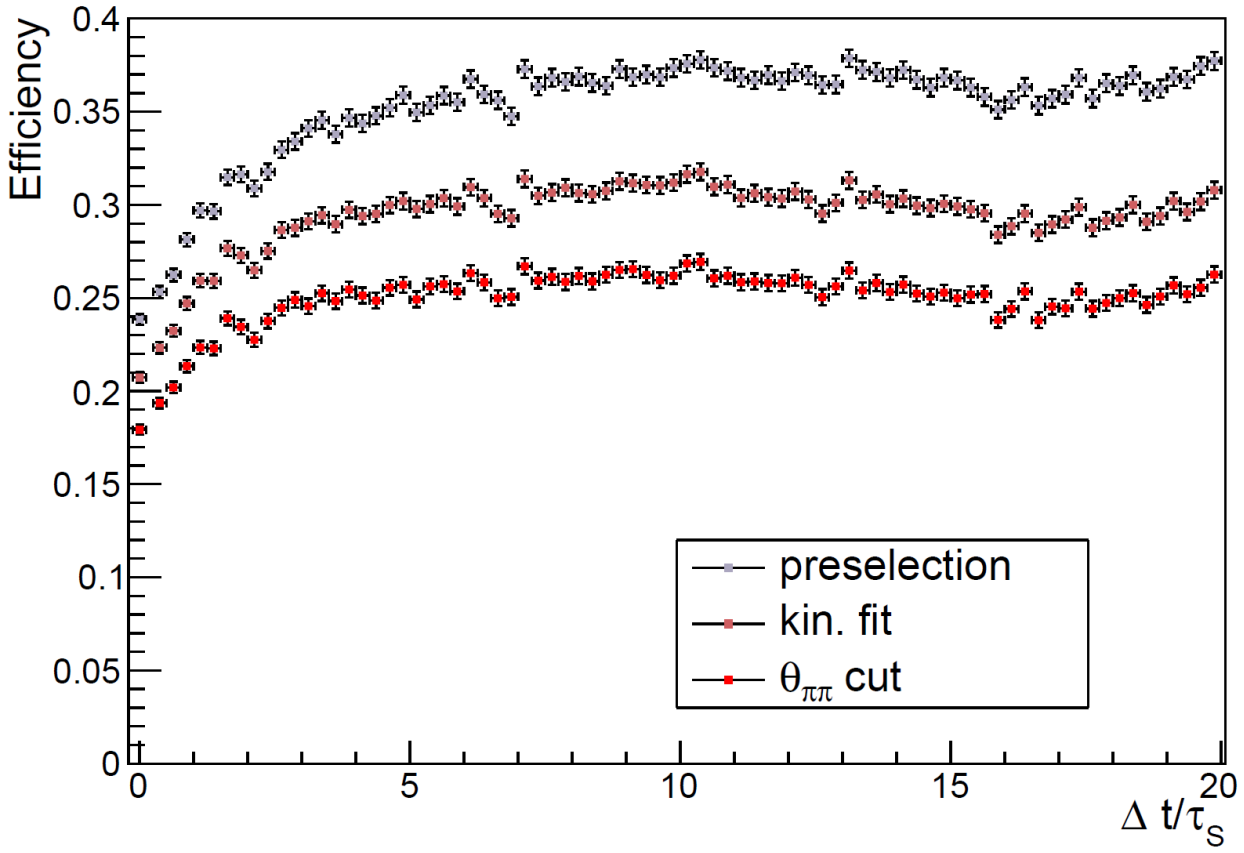

$$\epsilon_{tot} = \epsilon_{trig}\epsilon_{reco}\epsilon_{cut}$$

ϵ_{tot} only dependence on Δt is crucial.

ϵ_{cut} derived from MC and is in average $\approx 25\%$ with a small drop at $\Delta t \approx 0$ due to:

- Longer extrapolation lenght for both tracks that enhances the probability to fail reconstruction.
- Possible swaps of tracks associated to two different vertices when $\Delta t \approx 0$

Data-Monte Carlo Correction

$\epsilon_{trig}\epsilon_{reco}$ provided by the MC are checked with data using an independent control sample of

$$K_S K_L \to \pi^+\pi^-\pi\mu\nu$$

Selected to have an high purity (95%). The correction was obtained by the ratio of the data and MC distributions.

A fit with a constant indicates a small average correction.

The resolution is parametrized as a 2D Smearing matrix derived from the $\Delta t^{true} vs\ \Delta t^{reco}$ distribution once properly normalized.

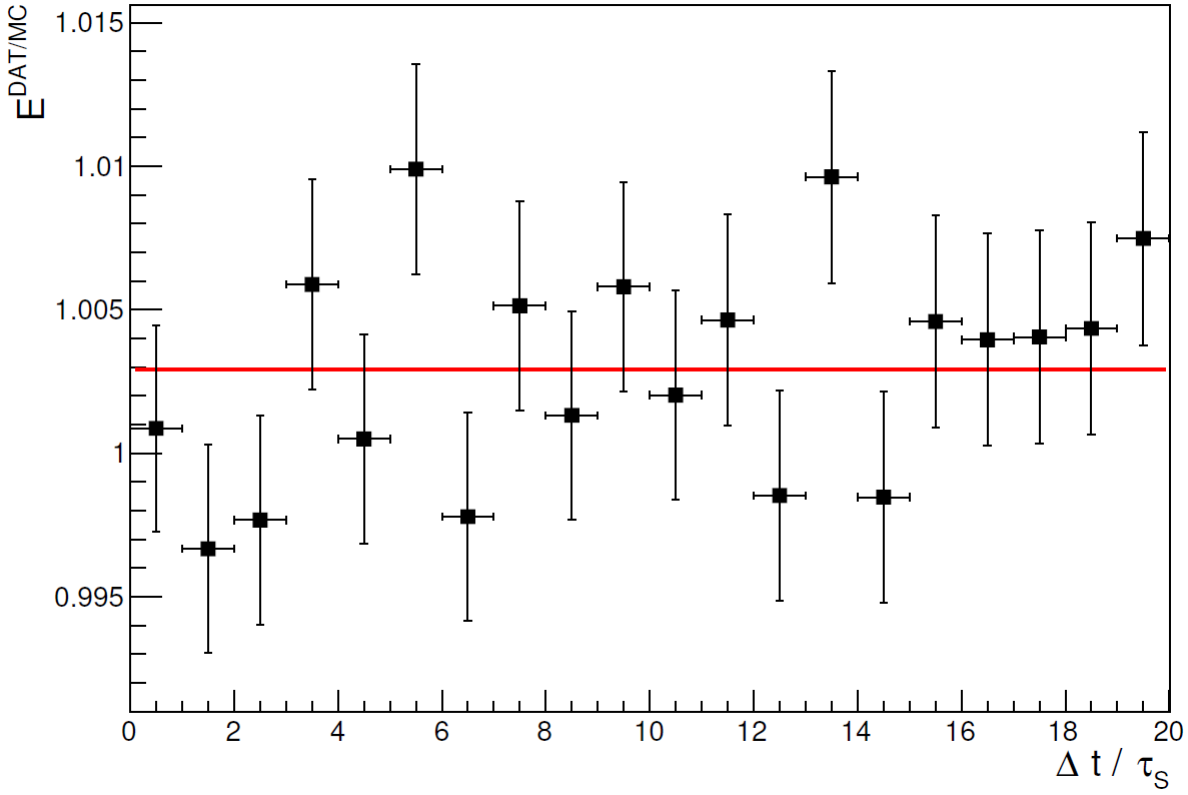

Fit procedure

$$N\left(\vec{\theta}\right)^{th}_{i} \doteq NE_i^{\frac{data}{MC}} \Sigma_j S_{i,j} R_j \epsilon_j I\left(\vec{\theta}\right)^{th}_{j}$$

Fit procedure

$$N\left(\vec{\theta}\right)^{th}_{i} \doteq NE_i^{\frac{data}{MC}} \Sigma_j S_{i,j} R_j \epsilon_j I\left(\vec{\theta}\right)^{th}_{j}$$

Decoherence parameter vector

Fit procedure

$$N\left(\vec{\theta}\right)^{th}_{i} \doteq NE_i^{\frac{data}{MC}} \Sigma_j S_{i,j} R_j \epsilon_j I\left(\vec{\theta}\right)^{th}_{j}$$

Cut Efficiency

Fit procedure

$$N\left(\vec{\theta}\right)^{th}_{i} \doteq NE_i^{\frac{data}{MC}} \Sigma_j S_{i,j} R_j \epsilon_j I\left(\vec{\theta}\right)^{th}_{j}$$

↑ Regeneration Correction

Fit procedure

$$N\left(\vec{\theta}\right)^{th}_{i} \doteq NE_i^{\frac{data}{MC}} \Sigma_j S_{i,j} R_j \epsilon_j I\left(\vec{\theta}\right)^{th}_{j}$$

Smearing Matrix

Fit procedure

$$N\left(\vec{\theta}\right)^{th}_{i} \doteq NE_i^{\frac{data}{MC}} \Sigma_j S_{i,j} R_j \epsilon_j I\left(\vec{\theta}\right)^{th}_{j}$$

Data-MC correction

Fit procedure

$$N\left(\vec{\theta}\right)^{th}_{i} \doteq NE_i^{\frac{data}{MC}} \Sigma_j S_{i,j} R_j \epsilon_j I\left(\vec{\theta}\right)^{th}_{j}$$

$$\chi^2 = \sum_{i=1}^{N_{bin}} \left(\frac{N_i^{Data} - N_i^{th}\left(\vec{\theta}\right)}{\sigma_i} \right)^2$$

To minimize

Fit procedure

$$N\left(\vec{\theta}\right)^{th}_{i} \doteq NE_i^{\frac{data}{MC}} \Sigma_j S_{i,j} R_j \epsilon_j I\left(\vec{\theta}\right)^{th}_{j}$$

$$\chi^2 = \sum_{i=1}^{N_{bin}} \left(\frac{N_i^{Data} - N_i^{th}\left(\vec{\theta}\right)}{\sigma_i} \right)^2$$

ζ_{SL} **Model**

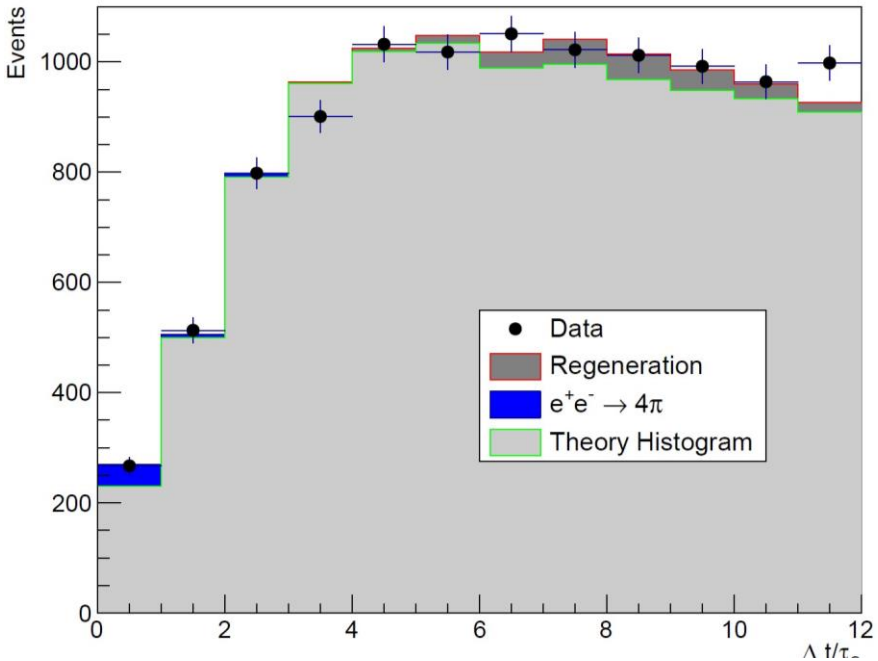

Systematic Analysis

To evalute the systematic uncertainty on the fit results the fitting procedure was repeated varying:

- **Selection cuts:** The cuts were varied according to their resolution σ to check the stability of the results.
- **Number of background events**
  - **4π Background:** Rescaling the number of background events according to the uncertainty of the total 4π backround $N_{bkg} = 51.0 \pm 5.7$
  - **Regeneration:** Varying the factor R_j according to $R_j' = R_j + \alpha(R_j - 1)$ with $-35\% < \alpha < 10\%$ depends on the knowledge of cross section ratio through the function $f(r)$.

Systematic Analysis

- **Δt resolution:** By enlarging and shrinking the smearing matrix $S_{i,j}$ using the relation:

$$\frac{\Delta t^{MC,true} - \Delta t'^{MC,reco}}{\Delta t^{MC,true} - \Delta t^{MC,reco}} = 1 + \delta k,$$

With $\delta k = \pm 0.75\%$

- **Physical constant:** Different sets of physical constants given in input to the theoretical models ($\tau_S, \tau_L, \Delta m$ and η_{+-}) are randomly generated according to their uncertainty and the fit repeated for each set. The standard deviation of the results is taken as systematic uncertainty.

Systematic Table

-	$\delta\zeta_{SL} \cdot 10^2$	$\delta\zeta_{0\bar{0}} \cdot 10^7$	$\delta\gamma \cdot 10^{21} GeV$	$\delta Re\omega \cdot 10^4$	$\delta \mathrm{Im}\omega \cdot 10^4$	$\delta\lvert\omega\rvert \cdot 10^4$	ϕ_ω(rad)
Cut stability	± 0.56	± 2.9	± 0.33	± 0.53	± 0.65	± 0.78	± 0.07
4π Background	± 0.37	± 1.9	± 0.22	± 0.32	± 0.19	± 0.32	± 0.04
Regeneration	± 0.17	± 0.9	± 0.10	± 0.06	± 0.63	± 0.58	± 0.05
Resolution	± 0.18	± 0.9	± 0.10	± 0.15	± 0.09	± 0.15	± 0.02
Phys. Const.	± 0.04	± 0.2	± 0.02	± 0.03	± 0.09	± 0.07	± 0.01
Total	$\mathbf{\pm 0.71}$	$\mathbf{\pm 3.7}$	$\mathbf{\pm 0.42}$	$\mathbf{\pm 0.64}$	$\mathbf{\pm 0.93}$	$\mathbf{\pm 1.04}$	$\mathbf{\pm 0.10}$

Conclusions: Results

$\mathbf{L = 1.7\ fb^{-1}}$

$\zeta_{SL} = (0.1 \pm 1.6_{stat} \pm 0.7\_syst) \cdot 10^{-2}$ → $\chi^2/ndf = 11.2/10$

$\zeta_{0\bar{0}} = \left(-0.05 \pm 0.80_{stat} \pm 0.37_{syst}\right) \cdot 10^{-6}$ → $\chi^2/ndf = 11.2/10$

$\gamma = \left(0.13 \pm 0.94_{stat} \pm 0.42_{syst}\right) \cdot 10^{-21}$ GeV → $\chi^2/ndf = 11.2/10$

$\Re\omega = (-2.3^{+1.9}_{-1.5_{stat}} \pm 0.6_{syst}) \cdot 10^{-4}$

$\Im\omega = (-4.1^{+2.8}_{-2.6_{stat}} \pm 0.9_{syst}) \cdot 10^{-4}$ → $\chi^2/ndf = 9.2/9$

$|\omega| = \left(4.7 \pm 2.9_{stat} \pm 1.0_{syst}\right) \cdot 10^{-4}$

$\phi_\omega = -2.1 \pm 0.2_{stat} \pm 0.1_{\mathrm{syst}}\ (\mathrm{rad})$ → $\chi^2/ndf = 9.2/9$

Conclusions: Results

$\Re\omega, \Im\omega$ *Model Contour Plot*

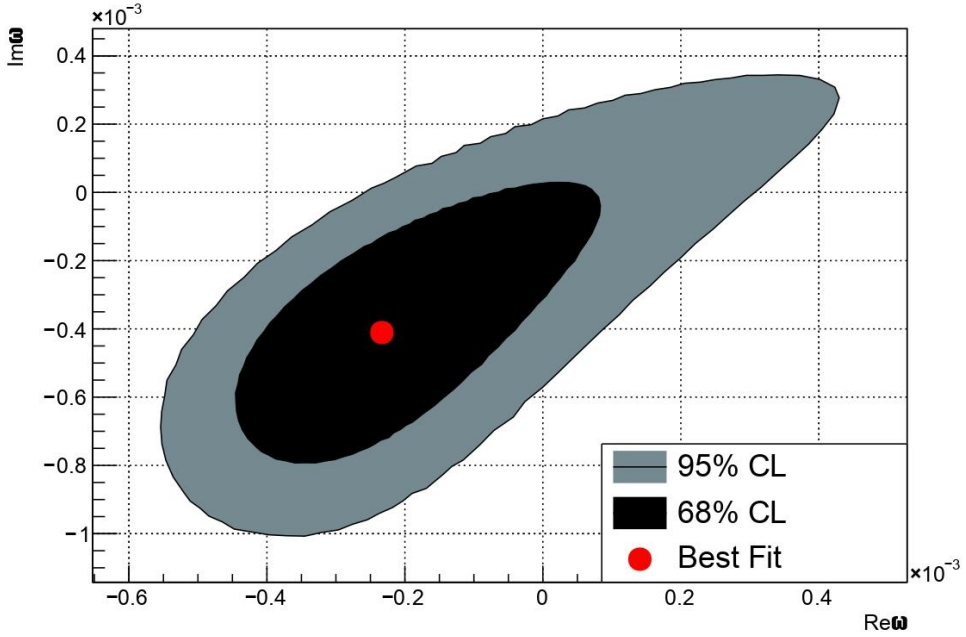

$|\omega|, \phi_\omega$ *Model Contour Plot*

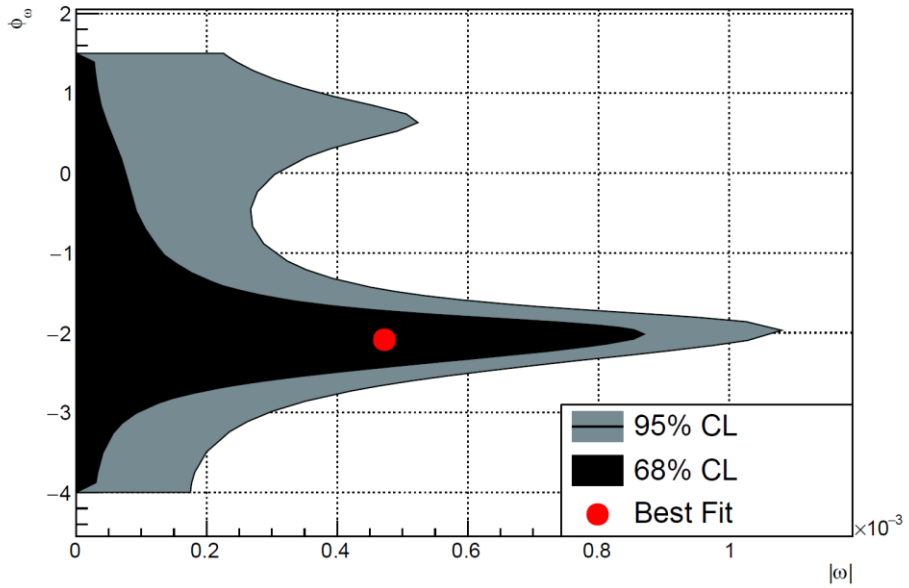

Conclusions: Results

$\Re\omega, \Im\omega$ *Model Contour Plot*

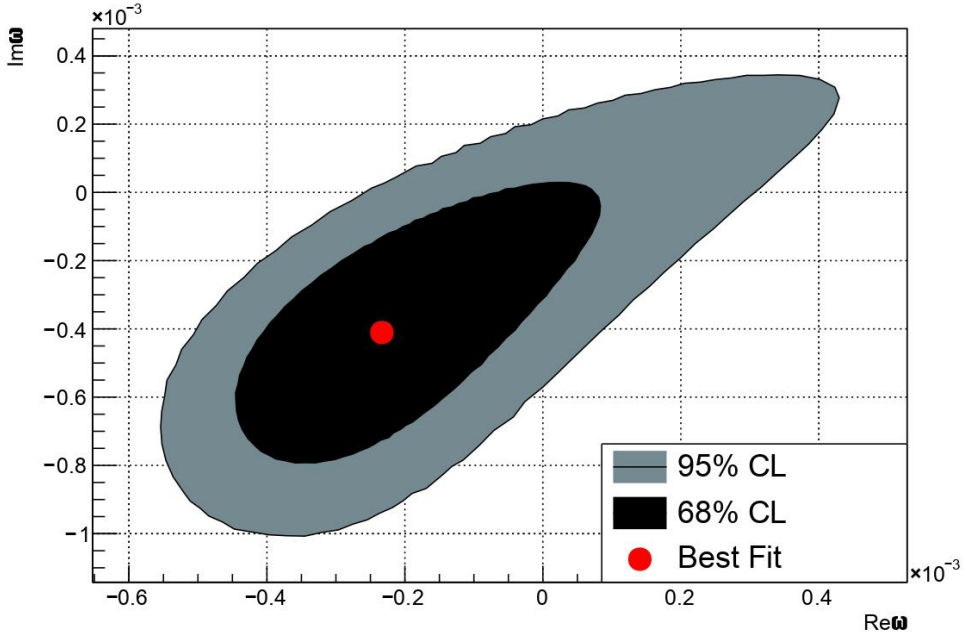

$|\omega|, \phi_\omega$ *Model Contour Plot*

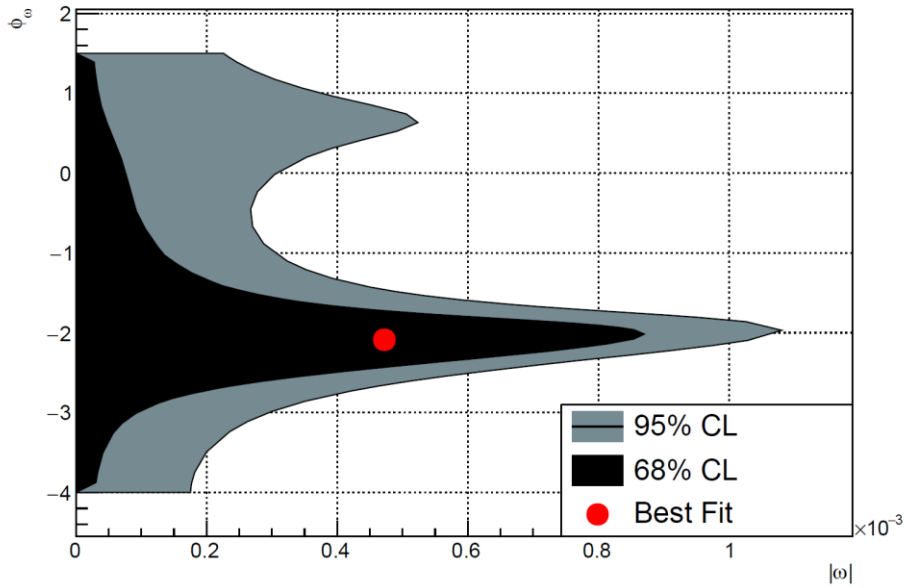

Statistical uncertainty reduced by more than half with respect to previous analysis
Central values consistent with zero → No decoherence and CPT violation
Results published on JHEP (2022) https://doi.org/10.1007/JHEP04(2022)059

Conclusions: Upper Limits

The results for $\zeta_{SL}, \zeta_{0\overline{0}}$ and γ, which are constrained to be > 0, can be translated into upper limits:

Conclusions: Upper Limits

The results for $\zeta_{SL}, \zeta_{0\bar{0}}$ and γ, which are constrained to be > 0, can be translated into upper limits:

New: $\mathbf{L = 1.7\ fb^{-1}}$

$$\zeta_{SL} < 0.028\ (90\%\ CL)$$
$$\zeta_{0\bar{0}} < 1.4 \cdot 10^{-6}\ (90\%\ CL)$$
$$\gamma < 1.8 \cdot 10^{-21}\ (90\%\ CL)$$

Conclusions: Upper Limits

The results for $\zeta_{SL}, \zeta_{0\bar{0}}$ and γ, which are constrained to be > 0, can be translated into upper limits:

New: $\mathbf{L = 1.7\ fb^{-1}}$

$$\zeta_{SL} < 0.028\ (90\%\ CL)$$
$$\zeta_{0\bar{0}} < 1.4 \cdot 10^{-6}\ (90\%\ CL)$$
$$\gamma < 1.8 \cdot 10^{-21}\ (90\%\ CL)$$

From the value of $|\omega|^2$ we can put an upper limit on $BR(\phi \to K_S K_S)$:

Conclusions: Upper Limits

The results for $\zeta_{SL}, \zeta_{0\bar{0}}$ and γ, which are constrained to be > 0, can be translated into upper limits:

New: L = 1.7 fb^{-1}

$$\zeta_{SL} < 0.028\ (90\%\ CL)$$
$$\zeta_{0\bar{0}} < 1.4 \cdot 10^{-6}\ (90\%\ CL)$$
$$\gamma < 1.8 \cdot 10^{-21}\ (90\%\ CL)$$

From the value of $|\omega|^2$ we can put an upper limit on $BR(\phi \to K_S K_S)$:

New: L = 1.7 fb^{-1}

$$BR(\phi \to K_S K_S) < 2.4 \cdot 10^{-7} (90\%\ C.L)$$

THANK YOU FOR THE ATTENTION